

Effect of Cutting Second-Order Chordae on In-Vivo Anterior Mitral Leaflet Compound Curvature

Filiberto Rodriguez¹, Frank Langer¹, Katherine B. Harrington¹, Frederick A. Tibayan¹, Mary K. Zasio¹, David Liang², George T. Daughters^{1,3}, Neil B. Ingels^{1,3}, D. Craig Miller¹

¹Department of Cardiothoracic Surgery and ²Division of Cardiovascular Medicine, Stanford University School of Medicine, Stanford, CA, ³Laboratory of Cardiovascular Physiology and Biophysics, Palo Alto Medical Foundation Research Institute, Palo Alto, CA, USA

Background and aim of the study: Leaflet curvature determines leaflet stress. In order to assess the influence of second-order chordae (2°CT) on anterior mitral valve leaflet (AMVL) geometry, AMVL curvature was measured before (Baseline) and after (CUT) cutting the 2°CT.

Methods: Miniature radiopaque markers were sutured onto the AMVL in eight sheep: four along the central-meridian from mid-septal annulus to the free-margin; and one each at the 2°CT insertion. Biplane videofluoroscopic data were acquired (open-chest) before and after CUT. Marker-triplet 3-D coordinates were used to calculate radii-of-curvature at LVP_{max} along the central-meridian (ROC_m) and across the AMVL belly (commissure-commissure axis, ROC_{c-c}).

Results: CUT did not change LVP_{max} (111 ± 12 versus 106 ± 11 mmHg; $p = 0.19$). At baseline, the AMVL central-meridian had compound curvature: Convex to the left ventricle near the annulus ($-ROC_m$) and concave near the free-margin ($+ROC_m$). After CUT, the AMVL flattened: ROC_m increased near the annulus (from -1.37 ± 0.52 to -12.58 ± 29.04 cm; $p = 0.02$), but

did not change near the edge. In the commissure-commissure axis, ROC_{c-c} was concave to the left ventricle at baseline and increased after CUT in all eight animals. In five sheep, ROC_{c-c} was increased (from 1.93 ± 1.01 to 2.80 ± 1.36 cm; $p = 0.03$), but in three sheep ROC_{c-c} was increased and inverted (from 3.65 ± 2.17 to -1.72 ± 0.53 cm; $p = 0.03$), becoming convex to the left ventricle.

Conclusion: Compound curvature along the AMVL central-meridian appears to be an intrinsic leaflet property that persists even without support from second-order chordae, whereas concave curvature in the commissure-commissure axis is more dependent on intact second-order chordae. Leaflet compound curvature must be incorporated into future finite element models to characterize leaflet stresses accurately. The importance of second-order chordae in maintaining leaflet shape must be considered during mitral repair. A larger ROC increases leaflet stresses, while reversal of ROC changes tensile stress to compressive stress; this might trigger deleterious leaflet remodeling after chordal cutting.

The Journal of Heart Valve Disease 2005;14:592-602

Two major sets of chordae radiate from the papillary muscles to support the mitral leaflets. First-order (primary or 'marginal') chordae insert on the leaflet free margins, while second-order chordae, which are larger and fewer in number, insert on the ventricular surface of the leaflets (1). In the anterior mitral valve leaflet (AMVL), two thicker basal (or 'strut') second-order chordae insert at the junction of the rough and smooth zones. Mitral leaflet curvature is an important deter-

minant of leaflet stress, and numerous mathematical models have related leaflet curvature to leaflet stress by Laplace's law (2-6). These studies describe the importance of leaflet curvature in minimizing leaflet stress, although they assume, based on ex-vivo findings, a passive mitral valve that billows during systole towards the left atrium (3-5). Radiopaque leaflet marker in-vivo sheep experiments, however, document a compound curvature along the central meridian of the AMVL, convex to the left ventricle, close to the annulus and concave near the leaflet margin (7,8). This compound curvature may reflect the normal insertion of second-order chordae into the AMVL belly, thereby establishing the convex curvature near the annulus, with the first-order chordae creating the concave curvature near the leaflet free margin. This compound leaflet shape has important implications in

Presented at the Third Biennial Meeting of the Society for Heart Valve Disease, 17th-20th June 2005, Vancouver Convention and Exhibition Centre, Vancouver, Canada

Address for correspondence:
D. Craig Miller MD, Department of Cardiothoracic Surgery, Falk Cardiovascular Research Center, Stanford University School of Medicine, Stanford, California 94305-5247, USA
e-mail: dcm@stanford.edu

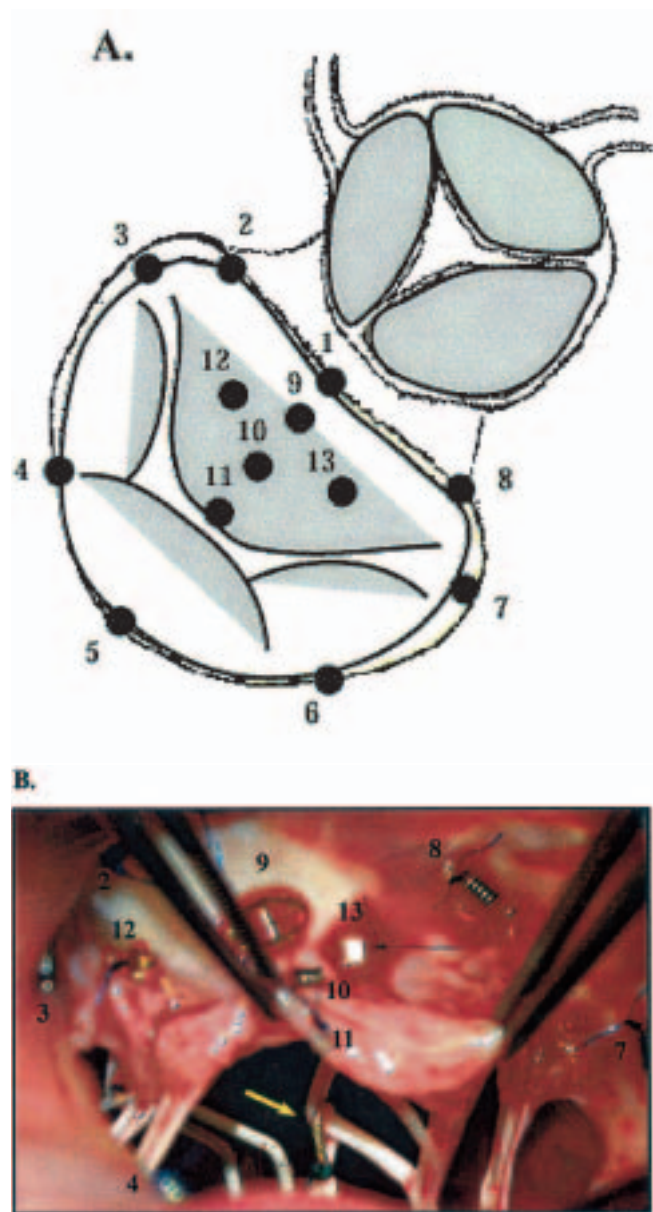


Figure 1: Anterior mitral leaflet marker array. A) Mitral annular and anterior leaflet markers. Eight miniature radiopaque markers were sutured around the mitral annulus (#1-8); marker #1 denotes the mid-septal annulus (the 'saddle horn'). Five markers were sutured on the anterior leaflet (#9-13), with three markers spaced evenly along the central meridian from the saddle horn to the leaflet edge (#9-11), and one marker sutured at the second-order chordae insertion-points (#12 and 13). B) Intraoperative photograph showing the anterior leaflet with sutured markers. Numbers correspond to marker labels. Arrow denotes a large, second-order 'strut' chord encircled with a wire snare. Smaller, first-order chordae can be seen inserting on the leaflet edge.

modeling leaflet stresses, since the portion of the leaflet that is convex to the left ventricle experiences compressive stress during systole, whereas the portion of the leaflet that is concave to the left ventricle experiences tensile stress.

Alterations in leaflet shape can trigger collagen synthesis (9,10), which might lead to compensatory leaflet thickening and altered leaflet mechanics, and perhaps limit the long-term durability of mitral valve repairs. The 10-year failure rates for valve repair in patients with myxomatous mitral valve disease range from 5% to 12% (11-13). Because many of these failures result from leaflet, chordal or suture line disruption, mechanical stress has been suggested as a causative factor (5,14). In contrast, in patients with chronic ischemic mitral regurgitation (IMR), the progression of MR to moderate-severe or greater after ring annuloplasty has been shown to be 25% within the first six months after repair (15), and five-year failure rates of up to 29% have been reported (15,16). These failures probably result from persistent systolic leaflet apical tethering caused by displacement of the papillary muscle (17-19) and progressive left ventricular (LV) remodeling that affects the entire subvalvular apparatus (20), which isolated ring annuloplasty cannot address.

Cutting the AMVL second-order chordae has been proposed as a therapeutic option for valve repair in patients with IMR to improve leaflet coaptation by reducing AMVL tethering (21,22). These experiments documented decreased leaflet angulation along the AMVL central-meridian after chordal cutting using echocardiography (21,22), which has also been confirmed with radiopaque marker studies (23), although leaflet curvature was not assessed. Chordal cutting, however, does not consistently eliminate or prevent IMR (23), and the abrupt change in AMVL shape after chordal cutting may increase leaflet stresses and trigger intrinsic leaflet remodeling that could potentially limit repair durability. Moreover, the importance of second-order chordae in preserving regional (24) and global (25) LV systolic pump function should be remembered.

The study aim was to characterize completely AMVL curvature in vivo and to determine the importance of the second-order chordae in maintaining leaflet shape. Radii of curvature (ROC), as defined by marker triplets, were calculated in order to quantify leaflet curvature along the central meridian and also across the leaflet belly in the commissure-commissure axis. This allowed testing of the hypothesis that chordal cutting affects leaflet curvature. Since leaflet curvature is a major determinant of leaflet stress, these changes were measured when LV pressure was highest, which corresponds to the time of maximal leaflet load.

Materials and methods

Animals

Twenty-two Dorsett-hybrid sheep (mean body weight 74 ± 10 kg) were used in these experiments. All animals received humane care in compliance with the Principles of Laboratory Animal Care formulated by the National Society for Medical Research and the Guide for Care and Use of Laboratory Animals prepared by the National Academy of Sciences and published by the National Institutes of Health (DHEW NIHG publication 85-23, revised 1985). This study was approved by the Stanford Medical Center Laboratory Research Animal Review committee and conducted according to Stanford University policy.

Surgical preparation

Each animal was premedicated with ketamine (25 mg/kg, i.m.), after which anesthesia was induced with sodium thiopental (6.8 mg/kg, i.m.) and maintained with inhalational isoflurane (1.5-2.2%). Through a left thoracotomy, the heart was suspended in a pericardial cradle. With the animal under cardiopulmonary bypass (CPB; mean time 80 ± 9 min) and using cardioplegic arrest (mean 60 ± 7 min) via a left atriotomy, eight miniature radiopaque markers were sutured around the mitral annulus (MA), starting at the mid-septal annulus ('saddle horn'), and five markers were sutured on the AMVL (Fig. 1A and B). Three AMVL markers were sutured down the central meridian of the leaflet, spaced evenly from the saddle horn to the leaflet free margin, and one marker was sutured at the insertion-point of each of the largest of the second-order chordae from each papillary muscle (i.e. the two most prominent 'strut' chordae). Wire snares (insulated except where they encircled the chordae) were secured around each strut chord (Fig. 1B) and exteriorized. Care was taken to ensure that no first-order chordae were trapped by the snares. A micromanometer-tipped catheter (Millar SPC-500; Millar Instruments, Inc., Houston, TX, USA) was inserted through the LV apex to monitor LV pressure (LVP). Animals were weaned from CPB and received intravenous magnesium sulfate (3 g), lidocaine (100 mg) and bretylium tosylate (50 mg) as prophylaxis against arrhythmias. Epicardial color Doppler echocardiography confirmed normal leaflet motion and valvular competence.

Experimental protocol

Immediately after surgery, the animals were transferred to the catheterization laboratory and studied with the chest open and anesthesia maintained with inhalational isoflurane (1.5-2.2%). Sequences of biplane videofluoroscopic and hemodynamic data

were acquired with animals in the right lateral decubitus position and ventilation arrested at end-expiration. Baseline data were acquired with the second-order chordae intact (Baseline). Before chordal cutting, animals received an additional 100 mg lidocaine (i.v.) as prophylaxis against rhythm disturbances. Animals were allowed to stabilize for 5 min, after which the strut chords were cut by passing an electrocautery current through the externalized wire snares. Data were then acquired immediately after chordal cutting (CUT). Simultaneous transesophageal color Doppler echocardiography allowed evaluation of the degree of MR before and after CUT by an experienced echocardiographer (D.L.) on a scale of 0 = none; 1 = mild; 2 = moderate; 3 = moderate-severe; 4 = severe).

Data acquisition

Videofluoroscopic images were recorded at 60 Hz using a Philips Optimus 2000 biplane Lateral ARC 2/poly DIAGNOST C2 system (Philips Medical Systems, Pleasanton, CA, USA). Two-dimensional images from the two X-ray views were digitized using custom software (26). These data were merged to yield three-dimensional (3-D) coordinates for each radiopaque marker every 16.7 ms, the accuracy of which is 0.1 ± 0.3 mm (27). Analog LVP and electrocardiogram signals were digitized simultaneously and recorded on videotape along with marker images during data acquisition.

Data analysis

Animal grouping

Only eight animals survived successful transection of both second-order strut chordae without damage to first-order chordae or the AMVL and without ventricular fibrillation during the cutting attempt; details have been reported previously (25). These eight animals comprised the present study group, and correct marker placement was confirmed on necropsy.

Leaflet radii of curvature

For the eight animals of the study group, hemodynamic and marker-derived data from three consecutive steady-state beats in sinus rhythm were time-aligned at LVPmax and averaged for each animal before (Baseline) and after (CUT) strut chord transection. In order to describe mitral leaflet 3-D geometry, marker coordinates were transformed from their original fixed laboratory reference to an internal, moving, right-handed Cartesian coordinate system (Fig. 2A) with origin at the centroid of the eight mitral annular markers (see Fig. 1A), the y-axis directed toward the LV apex, the x-axis toward the lateral LV wall (marker #5), and the z-axis toward the posteromedial mitral commissure (marker #7). The 3-D plot (Fig. 2A) shows

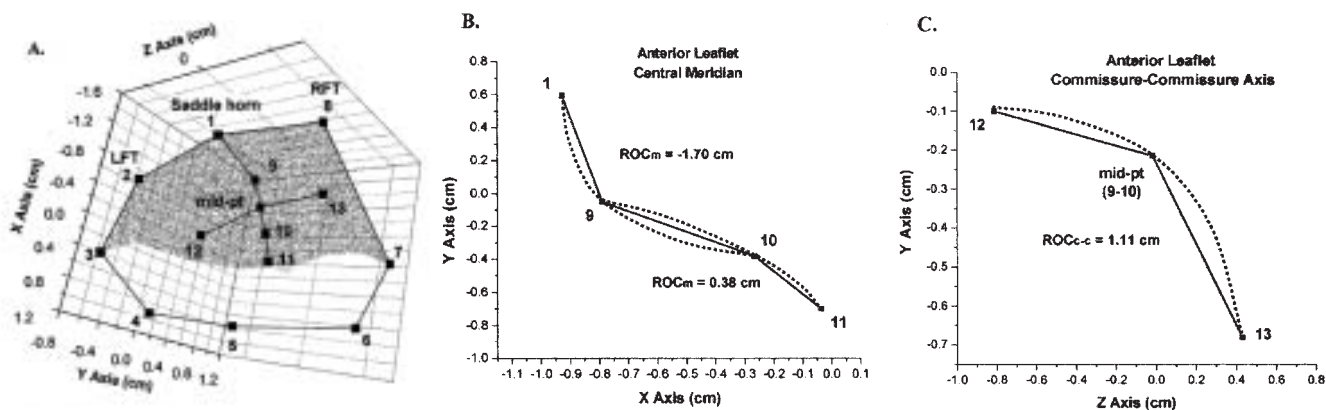


Figure 2: Leaflet marker geometry. A) Marker coordinates were transformed from their original fixed laboratory reference frame to an internal right-handed Cartesian coordinate system. This 3-D plot shows anterior leaflet and mitral annular marker positions at maximum left ventricular pressure (LVP_{max}) from a representative animal at baseline. The shaded area denotes the anterior leaflet. Numbers correspond with marker labels as shown in Fig. 1. LFT: Left fibrous trigone; RFT: Right fibrous trigone; 'mid-pt' denotes the midpoint between markers 9 and 10 in this animal. B) Anterior leaflet central meridian 2-D marker positions at LVP_{max} from the same representative animal projected onto the lateral (x) - apical (y) plane at baseline. Two radii of curvature (ROC_m), which characterize the anterior leaflet central meridian shape, were calculated using the (x) and (y) coordinates of the four markers from the mid-septal annulus to the leaflet free-edge. Markers #1, 9 and 10 define the 'proximal' ROC_m near the mitral annulus, and markers #9, 10 and 11 define the 'distal' ROC_m near the leaflet edge. Arcs schematically represent portions of circumscribed circles used to calculate leaflet ROC. The anterior mitral leaflet central meridian shows compound curvature: convex to the left ventricle near the annulus ($-ROC_m$) and concave near the leaflet edge ($+ROC_m$). C) Anterior leaflet 2-D marker positions in the commissure-commissure axis at LVP_{max} from the same representative animal projected onto the orthogonal (z) - apical (y) plane at baseline. One radius of curvature (ROC_{c-c}) was calculated across the leaflet belly in the commissure-commissure axis using the (z) and (y) coordinates of the markers spanning the second-order chordal insertions. The arc schematically represents a portion of the circumscribed circle used to calculate leaflet ROC in this direction. At baseline, curvature of the anterior mitral leaflet in the commissure-commissure axis is concave to the left ventricle ($+ROC_{c-c}$). Numbers correspond to marker labels; 'mid-pt' denotes the midpoint between markers 9 and 10 in this animal (see Materials and methods).

the anterior leaflet shape at baseline from a representative animal, with annular and leaflet markers corresponding with those from Figure 1.

Anterior leaflet ROC were calculated from marker triplets. Each marker triad defines an arc of a unique circle, the radius of which is the ROC (Fig. 3). The equation of the circle given by three points [$P_1(x_1, y_1)$, $P_2(x_2, y_2)$, $P_3(x_3, y_3)$] is:

$$R_2 = (x - x_M)^2 + (y - y_M)^2$$

where R is the radius of the circle, and:

$$x_M = [(r_1^2 - r_2^2)(y_2 - y_3) - (y_1 - y_2)(r_2^2 - r_3^2)] / 2[(x_1 - x_2)(y_2 - y_3) - (y_1 - y_2)(x_2 - x_3)]$$

$$y_M = [(r_1^2 - r_2^2)(x_2 - x_3) - (x_1 - x_2)(r_2^2 - r_3^2)] / 2[(y_1 - y_2)(x_2 - x_3) - (x_1 - x_2)(y_2 - y_3)]$$

where:

$$r_1^2 = x_1^2 + y_1^2$$

$$r_2^2 = x_2^2 + y_2^2$$

$$r_3^2 = x_3^2 + y_3^2$$

Two ROCs were calculated along the AMVL central meridian (ROC_m) using the (x) and (y) coordinates of the four markers (Fig. 2B). Markers #1, 9 and 10 defined the 'proximal' ROC_m near the MA, while markers #9, 10 and 11 defined the 'distal' ROC_m near the leaflet free margin. One ROC orthogonal to the central meridian was calculated across the AMVL belly in the commissure-commissure direction (ROC_{c-c}) using the (z) and (y) coordinates of three marker points spanning the second-order chordal insertions (Fig. 2C). As the central meridian markers were first spaced evenly (markers #9-11; see Fig. 1), minor variations in the location of the two markers defining the second-order chordal insertions (#12 and 13; see Fig. 1) occurred based on individual anatomy. In three animals, the sec-

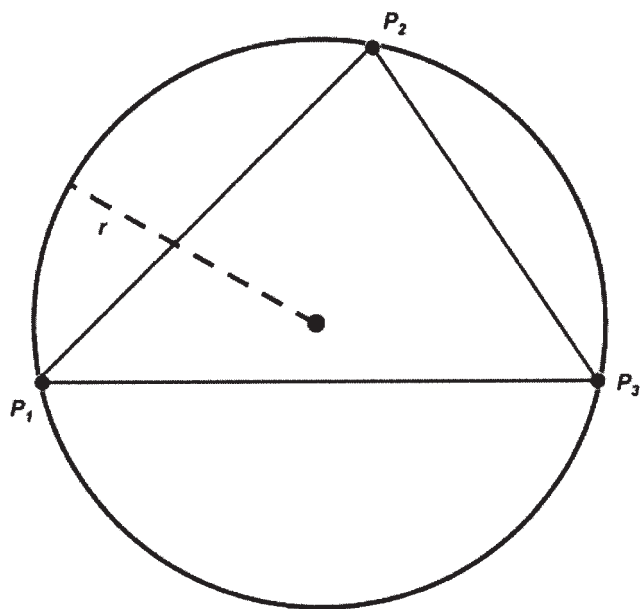


Figure 3: Calculating the radius of curvature. Each marker triad (P_1, P_2, P_3) defines an arc of a unique circle, the radius (r) of which is the radius of curvature (ROC). Anterior mitral leaflet ROCs were derived from marker triplet coordinates, which were used to calculate the equation of the circle given by the three points (see Materials and methods).

ond-order chordae insertions were in-line with marker #9; in one animal, the second-order chordae insertions were in-line with marker #10; and in four animals, second-order chordae insertions were between markers #9 and 10. Since the three points used to calculate ROC must be in-line, the coordinates of the midpoint between markers #9 and 10 were used for calculation of ROC in these four animals (Fig. 2; see also Fig. 5). Employing this derived midpoint is reasonable because the distance between these two markers (#9 and 10) is much less than the ROC, and the leaflet is nearly linear between these two markers.

Statistical analysis

All data were reported as mean \pm SD. The Kolmogorov-Smirnov test was used to test data for normal distribution. Baseline and CUT data that fitted a normal distribution were compared using Student's t-test for paired observations. Data that failed normality and also categorical data (e.g. degree of MR) were analyzed using the Wilcoxon Signed-Rank non-parametric test. All statistical analysis was performed using SigmaStat, v.2.03, and the level of significance was chosen as $p < 0.05$.

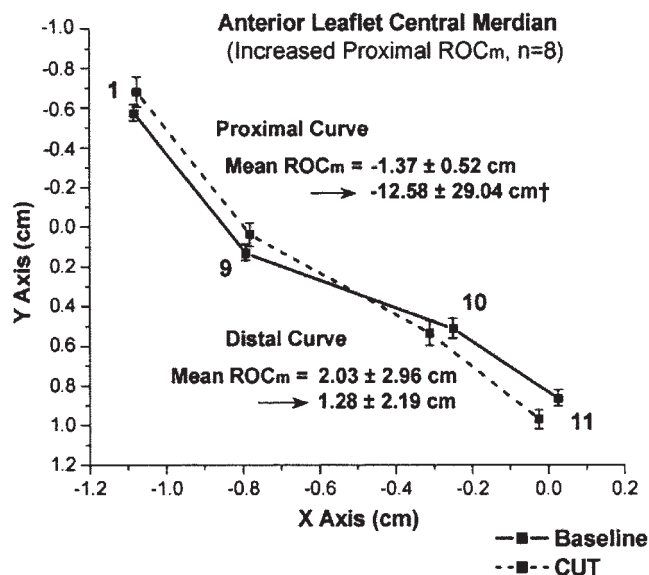


Figure 4: Anterior leaflet central meridian. Group mean marker positions (± 1 SE) are shown at maximum left ventricular (LV) pressure projected onto the lateral (x) - apical (y) plane at baseline (solid) and after chordal cutting (CUT, dashed). Two radii of curvature (ROC_m) were calculated along the anterior leaflet central meridian using the (x) and (y) coordinates of the four markers from the mid-septal annulus to the leaflet free-edge. Numbers correspond to marker labels. Markers #1, 9 and 10 define the 'proximal' ROC_m near the mitral annulus, and markers #9, 10 and 11 define the 'distal' ROC_m near the leaflet edge. Both before and after chordal cutting, the anterior mitral leaflet shows compound curvature: convex to the left ventricle near the annulus ($-ROC_m$) and concave near the leaflet edge ($+ROC_m$). Chordal cutting was associated with leaflet flattening and increased proximal ROC_m , although distal ROC_m did not change. ROC values are shown as mean ± 1 SD; † $p < 0.05$ versus Baseline; Wilcoxon Signed Rank test.

Results

Trace to mild MR was detected at baseline before chordal cutting, and there was no change in the degree of MR after transection of the second-order strut chordae (0.4 ± 0.4 (Baseline) versus 0.6 ± 0.4 (CUT); $p = NS$). Chordal cutting did not change LVPmax (111 ± 12 versus 106 ± 11 mmHg; $p = 0.19$). Figure 4 illustrates group mean data for the AMVL central meridian marker coordinates at LVPmax. Both before and after chordal cutting, the AMVL central meridian had a compound curvature: Convex to the left ventricle near the annulus ($-ROC_m$) and concave near the leaflet edge ($+ROC_m$). After chordal cutting, the AMVL became flatter, as reflected by increased proximal

Table I: Anterior leaflet radii of curvature.

Location	Baseline	CUT	p-value
Proximal central meridian (cm) (n = 8)	-1.37 ± 0.52	-12.58 ± 29.04 [†]	0.02
Distal central meridian (cm) (n = 8)	2.03 ± 2.96	1.28 ± 2.19	0.98
Commissure-commissure axis (cm) (n = 5)	1.93 ± 1.01	2.80 ± 1.36 [*]	0.03
Commissure-commissure axis (cm) (n = 3)	3.65 ± 2.17	-1.72 ± 0.53 [*]	0.03

[†]p <0.05 versus Baseline, Wilcoxon Signed-Rank test.

^{*}p <0.05 versus Baseline, Student's *t*-test for paired observations.

ROCM near the annulus and an unchanged distal ROCm near the leaflet edge. Figure 5 illustrates the AMVL marker coordinates at the second-order chordae insertion points in the commissure-commissure axis at LVPmax for all eight animals. At baseline, leaflet curvature in the commissure-commissure direction was concave to the LV (+ROCC-c). Chordal cutting was associated with increased ROCC-c in all eight animals; in five animals ROCC-c was increased, whilst in three others ROCC-c was increased and inverted, becoming convex to the left ventricle (-ROCC-c) after chordal cutting (Fig. 5). The group mean data of leaflet ROCs at baseline and after transection of the second-order chordae are summarized in Table I.

Discussion

Curvature is a fundamental component of the shape - and thereby stress - on the mitral leaflet. Hence, leaflet curvature is an important element of normal valve function. The findings from the present study reveal new and more complete in-vivo data that support several conclusions. First, at baseline, the anterior leaflet shape during systole at LVPmax is complex; the central meridian has a sigmoid shape that is convex to the left ventricle near the annulus and concave near the leaflet edge with a concave curvature in the commissure-commissure axis. Second, although chordal cutting resulted in flattening of the AMVL with increased central meridian ROCm near the annulus, the compound curvature along the AMVL central meridian persisted, even without support from second-order chordae. Third, concave curvature in the commissure-commissure axis appears to be more dependent on the second-order chordae as chordal cutting resulted in flattening and even inversion of AMVL curvature in the commissure-commissure axis. This complex compound curvature must be incorporated into future finite element models to estimate leaflet stresses accurately. The importance of second-order chordae in maintaining normal leaflet shape should be considered when performing valve repair. A larger ROC after chordal cutting would be expected to

increase leaflet stress, and reversal of curvature across the AMVL belly changes tensile stress to compressive stress in the leaflet. These changes may possibly trigger deleterious leaflet remodeling after chordal cutting.

Leaflet geometry at baseline

Existing mitral valve finite element and other mathematical models of leaflet stress during systole consider the leaflets as passive membranes with an elliptical, 'billowing' shape concave to the left ventricle (2,3,5,6,28). These leaflet shapes were derived from casts of excised hearts *ex vivo* (4). In contrast, miniature radiopaque markers provide the spatial and temporal resolution necessary to define leaflet shape in vivo more precisely. Consistent with the findings previously described by Karlsson et al. (7), which were obtained using a denser AMVL central meridian marker array, the normal anterior leaflet central meridian was found to adopt a compound shape in vivo at LVPmax, with a proximal curve convex to the left ventricle and a distal curve concave to the left ventricle (Figs. 2 and 4). Using a similar four-marker central meridian leaflet array, Tibayan et al. also recently described this AMVL compound shape (8). This compound leaflet shape has important implications for studies seeking to model leaflet stresses, because the portion of the leaflet that is convex to the left ventricle experiences compressive stress during systole, whereas the portion of the leaflet that is concave to the ventricle experiences tensile stress. The proximal bend, maintained convex to the ventricle even under maximum systolic pressures, is likely to be due to the interplay of forces between the annulus, leaflet, and also the second-order chordae that insert into the AMVL belly at the junction of the rough and smooth zones (7). The distal leaflet then assumes a concave curvature along the central meridian due to the insertion of first-order chordae on the leaflet free margin.

By also placing markers on the AMVL second-order chordae insertion points, the orthogonal curvature across the AMVL belly in the commissure-commissure axis could be further defined; this was concave to the

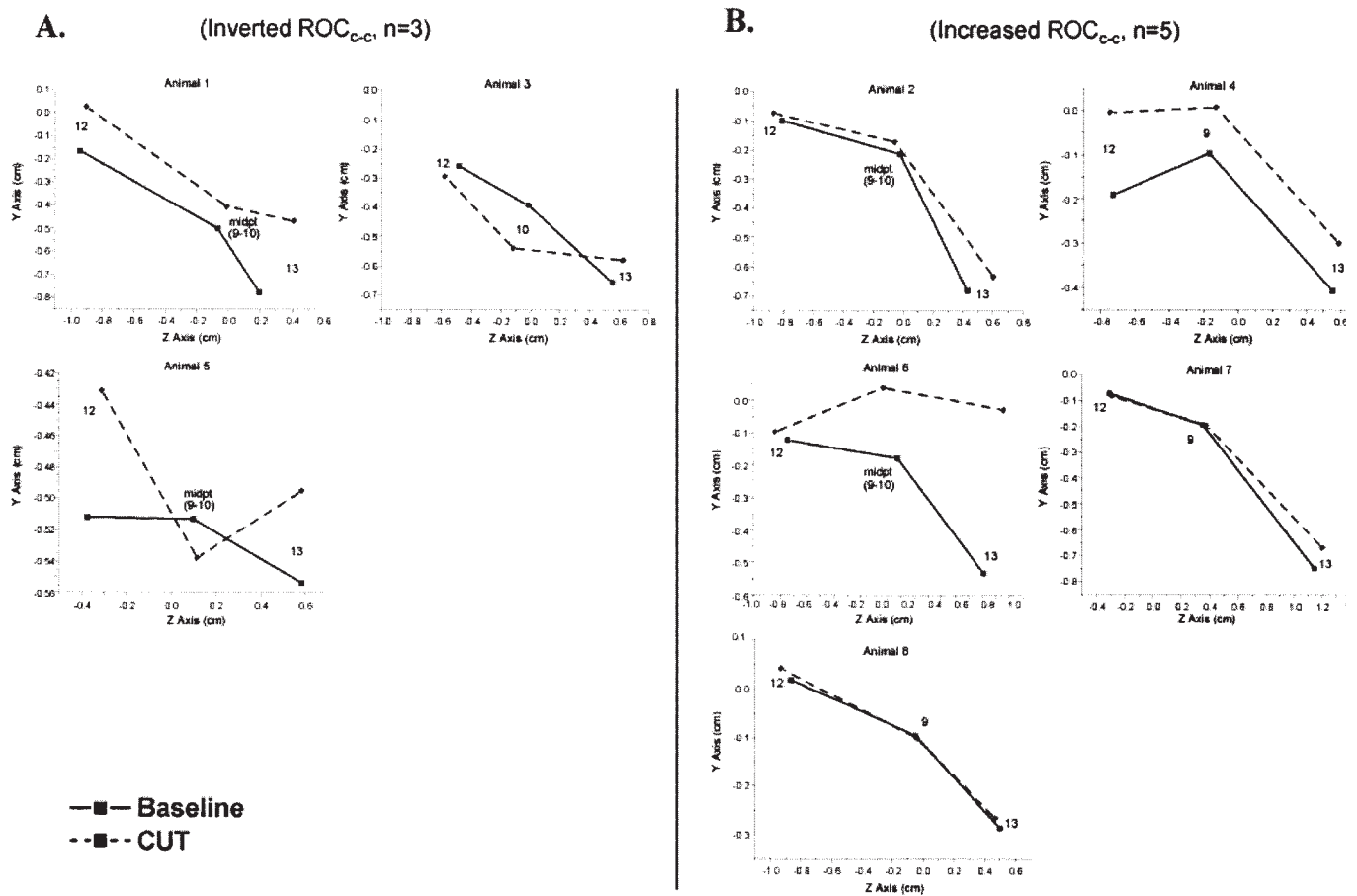


Figure 5: Anterior leaflet commissure-commissure axis. Marker positions are shown at maximum left ventricular (LV) pressure for each animal projected onto the orthogonal (z) - apical (y) plane at baseline (solid) and after chordal cutting (CUT, dashed). One radius of curvature (ROC_{c-c}) was calculated across the leaflet belly in the commissure-commissure axis using the (z) and (y) coordinates of the markers spanning the second-order chord insertions. Numbers correspond to marker labels, and 'mid-pt' refers to the central meridian marker coordinates used for calculation of orthogonal ROC_{c-c} (see Materials and methods). At baseline, curvature of the anterior mitral leaflet in the commissure-commissure axis was concave to the left ventricle in all hearts (+ ROC_{c-c}). Chordal cutting was associated with increased ROC_{c-c} in all eight animals. A) In three animals, ROC_{c-c} increased and inverted, becoming convex to the left ventricle (- ROC_{c-c}). B) In five animals, ROC_{c-c} increased but remained concave to the left ventricle (+ ROC_{c-c}). ROC values are shown as mean \pm 1 SD; * $p < 0.05$ versus Baseline; Student's t-test for paired observations.

left ventricle at baseline with the second-order chordae intact (Figs. 2 and 5). A concave cross-leaflet curvature may have physiologic advantages in terms of minimizing systolic leaflet stresses (5). Goetz and colleagues (29) also noted the systolic outflow funnel mechanism created by this concave cross-leaflet curvature, which it is believed may be enhanced by the sigmoid shape of the AMVL central meridian; all of this helps direct blood out via the LV outflow tract.

Changes in leaflet curvature after chordal cutting

In addition to precise characterization of normal leaflet shape in vivo, the leaflet markers allowed quan-

tification of leaflet curvature in the beating heart by calculating ROC from marker triplets. In thin membranes such as the mitral leaflets, curvature is related to stress according to the law of Laplace, namely that a larger radius of curvature accentuates leaflet stress. By measuring changes in leaflet curvature, it was hoped to predict the direction of changes in leaflet stress after transection of the second-order strut chordae.

After chordal cutting, the proximal ROC_m along the AMVL central meridian increased but the distal ROC_m did not change (Fig. 4). Compound leaflet shape, however, was preserved after chordal cutting, suggesting that this may be an intrinsic feature of the

AMVL and the geometry of the valvular-ventricular complex. Although the compound shape was preserved, chordal cutting did flatten the AMVL and increased the leaflet ROCm near the annulus. The original studies which proposed chordal cutting as a therapeutic treatment of IMR (21,22) described improved leaflet coaptation after chordal cutting by eliminating the echocardiographic bend or 'knee' in the AMVL - that is, the leaflet inflection angle, created by second-order chordal tethering. Leaflet flattening after chordal cutting, however, does not necessarily increase effective leaflet length (measured from the annulus to the leaflet edge), nor does it eliminate IMR (23). An increased ROCm, however, would tend to increase leaflet stress after chordal cutting.

Changes in the orthogonal, cross-leaflet curvature along the second-order chordae insertion sites also demonstrated complex perturbations in leaflet shape after chordal cutting in some animals. Chordal cutting increased orthogonal, cross-leaflet ROCC-c in all eight sheep, but ROCC-c increased, changed sign, and became convex to the left ventricle in three animals (Fig. 5). In the three animals where orthogonal ROCC-c became convex, the ROCC-c was larger at baseline than in the other five animals in which ROCC-c increased but did not reverse (Fig. 5; Table I). The larger cross-leaflet ROCC-c at baseline in the three animals in which ROCC-c reversed after chordal cutting may reflect that the AMVL was under higher stress at baseline in these animals, which may explain why ROCC-c reversed. This finding may underscore the importance of second-order chordae as support structures during conditions of high LV loading.

Increased leaflet ROC after chordal cutting will likely augment leaflet stresses, and curvature reversal would change tensile stress to compressive stress. Alterations in leaflet stress have been shown to up-regulate collagen synthesis (9), which could lead to compensatory leaflet thickening. While increased leaflet thickness may help to normalize leaflet stress, computer models suggest that it may also decrease leaflet mobility, thereby eventually exacerbating malcoaptation, possibly increasing MR, and producing further ventricular remodeling in a vicious cycle (10). Such leaflet remodeling has recently been described in patients with congestive heart failure (CHF) and functional MR (30). Although conventional wisdom has held that although LV chamber size and mitral annular diameter become larger in patients with CHF, the structure and composition of the mitral valve leaflets remain normal, Grande-Allen et al. (30) found that mitral leaflets from patients with CHF have increased cellularity and different extracellular matrix composition, including an increase in collagen content and glycosaminoglycans. Further alterations in leaflet stress

caused by increased ROCs and curvature reversal may exacerbate such leaflet remodeling and limit the durability of chordal cutting repairs in patients with IMR.

The changes in leaflet geometry observed in the present study contrast with earlier findings reported by the present authors' laboratory, in which no change in AMVL shape was found after transection of the second-order chordae (31). This may be explained by the fact that the older experimental preparation, as reported by Timek et al. (31) involved a much more complex and very long surgical procedure where the strut chordae were transected intraoperatively and then re-approximated with interposed strain gauges before 'control' data were obtained. Changes in systolic 3-D AMVL shape were then compared by statistical analysis of the leaflet marker (x), (y) and (z) coordinates near, but not at, LVPmax (31), and ROC were not determined. Hence, data regarding leaflet shape from these earlier experiments must be interpreted with caution because 'control' data were acquired after the second-order chordae had already been transected and re-approximated during a very long aortic cross-clamp interval, leaflet curvature was not assessed, and the data were not compared at LVPmax (the time of maximum leaflet load). In the present experiment, leaflet curvature was measured at LVPmax, and the experimental design allowed for paired, sequential comparisons between Baseline and CUT conditions without any antecedent chordal manipulations.

Study limitations

As the present data were obtained in an acute, open-chest setting in normal sheep hearts immediately after CPB, caution must be exercised when extrapolating these findings to humans with chronic ischemic heart disease. Nevertheless, the results demonstrate the compound anterior leaflet shape in vivo and the influence of second-order chordae. One potential concern was that the measured curves depended on the number and location of the markers; however, similar compound curvature was previously documented in experiments with more markers placed along the AMVL central meridian (7). Moreover, compound leaflet curvature has also been reported in closed-chest animals with and without chronic IMR (8). The ROC measurement is based on fitting a circular arc to three markers, although the true leaflet shape may be different from this fitted arc. Since the plane of the three markers is mostly perpendicular to the leaflet surface, curvature of the arc is a mean value with the true shape having less curvature at some places and more curvature at others. Thus, the measured ROC is the true ROC at least somewhere in the leaflet between the three markers. Although no stresses were directly measured or modeled in the present experiment, the

quantitative leaflet radii of curvature allows precise leaflet geometry to be determined in-vivo, and thereby to predict how geometric changes may alter leaflet stresses after chordal cutting.

In conclusion, the leaflet marker array used for the present analysis allowed the shape of the anterior mitral leaflet to be determined more completely during baseline conditions, which is compound along the central meridian and concave to the left ventricle in the commissure-commissure direction. These more complete quantitative in-vivo data should be considered in future computational models of mitral leaflet stress and valvular structure and function. Goetz et al. (29) called for a "...conscious respect for the integrity of the whole submitral apparatus." The specific role of the second-order chordae for mediating valvular-ventricular interaction has also been highlighted, demonstrating that there probably is a real price to pay in terms of depressing LV systolic function if the second-order chordae are divided (24,25). The findings from the present analysis add an additional price of chordal cutting in terms of perturbing normal leaflet curvature, in that larger ROC along the proximal AMVL central meridian and orthogonally in the commissure-commissure leaflet axis would be expected to increase leaflet stress. Moreover, reversal of ROCc-c across the AMVL belly changes tensile stress to compressive stress, which may trigger leaflet tissue remodeling and perhaps even limit repair durability after chordal cutting in patients with IMR.

Acknowledgements

The authors appreciate the superb technical assistance provided by Carol W. Mead, Maggie Brophy, Katha Gazda and Mark Grisedale. They also thank John C. Criscione for his bioengineering expertise. These studies were supported financially by Grants HL-29589 and HL-67025 from the National Heart, Lung and Blood Institute. Drs. Rodriguez, Langer and Tibayan were Carl and Leah McConnell Cardiovascular Surgical Research Fellows. Dr. Rodriguez was supported by Grant HL67025-01S1 from the NHLBI and was also a recipient of an American College of Surgeons Resident Research Scholarship Award. Dr. Langer was supported by the Deutsche Akademie der Naturforscher Leopoldina, and Dr. Tibayan was supported by NHLBI Individual Research Service Award HL-67563.

References

1. Lam, JHC, Ranaganthan, N, Wigle, ED, et al. Morphology of the human mitral valve: I. Chordae tendinae: A new classification. *Circulation* 1970;41:449
2. Mazumdar J, Hearn TC. Mathematical analysis of mitral valve leaflets. *J Biomech* 1978;11:291-296
3. Arts T, Meerbaum S, Reneman R, Corday E. Stresses in the closed mitral valve: A model study. *J Biomech* 1983;16:539-547
4. Kunzelman KS, Cochran RP, Chuong C, Ring WS, Verrier ED, Eberhart RD. Finite element analysis of the mitral valve. *J Heart Valve Dis* 1993;2:326-340
5. Salgo IS, Gorman JH, III, Gorman RC, et al. Effect of annular shape on leaflet curvature in reducing mitral leaflet stress. *Circulation* 2002;106:711-717
6. Lim KH, Yeo JH, Duran CMG. Three-dimensional asymmetrical modeling of the mitral valve: A finite element study with dynamic boundaries. *J Heart Valve Dis* 2005;14:386-392
7. Karlsson MO, Glasson JR, Bolger AF, et al. Mitral valve opening in the ovine heart. *Am J Physiol* 1998;274(2 Pt.2):H552-H563
8. Tibayan FA, Rodriguez F, Langer F, et al. Increases in mitral leaflet radii of curvature with chronic ischemic mitral regurgitation. *J Heart Valve Dis* 2004;13:772-778
9. Quick DW, Kunzelman KS, Kneebone JM, Cochran RP. Collagen synthesis is upregulated in mitral valves subjected to altered stress. *Am Soc Artif Intern Organs J* 1997;43:181-186
10. Kunzelman KS, Quick DW, Cochran RP. altered collagen concentration in mitral valve leaflets: Biochemical and finite element analysis. *Ann Thorac Surg* 1998;66(6 Suppl.):S198-S205
11. Cohn LH, DiSesa VJ, Couper GS, Peigh PS, Kowalker W, Collins JJ, Jr. Mitral valve repair for myxomatous degeneration and prolapse of the mitral valve. *J Thorac Cardiovasc Surg* 1989;98(5 Pt.2):987-992
12. David TE, Armstrong S, Sun Z, Daniel L. Late results of mitral valve repair for mitral regurgitation due to degenerative disease. *Ann Thorac Surg* 1993;56:7-12
13. Braunberger E, Deloche A, Berrebi A, et al. Very long-term results (more than 20 years) of valve repair with Carpentier's techniques in non-rheumatic mitral valve insufficiency. *Circulation* 2001;104(12 Suppl.1):I8-I11
14. Gillinov AM, Cosgrove DM, Blackstone EH, et al. Durability of mitral valve repair for degenerative disease. *J Thorac Cardiovasc Surg* 1998;116:734-743
15. McGee EC, Gillinov AM, Blackstone EH, et al. Recurrent mitral regurgitation after annuloplasty for functional ischemic mitral regurgitation. *J Thorac Cardiovasc Surg* 2004;128:916-924
16. Tahta SA, Oury JH, Maxwell JM, Hiro SP, Duran CM. outcome after mitral valve repair for functional ischemic mitral regurgitation. *J Heart Valve Dis* 2002;11:11-18

17. Otsuji Y, Handschumacher MD, Schwammenthal E, et al. Insights from three-dimensional echocardiography into the mechanism of functional mitral regurgitation: Direct in vivo demonstration of altered leaflet tethering geometry. *Circulation* 1997;96:1999-2008
18. Yiu SF, Enriquez-Sarano M, Tribouilloy C, Seward JB, Tajik AJ. Determinants of the degree of functional mitral regurgitation in patients with systolic left ventricular dysfunction: A quantitative clinical study. *Circulation* 2000;102:1400-1406
19. Tibayan FA, Rodriguez F, Zasio MK, et al. Geometric distortions of the mitral valvular-ventricular complex in chronic ischemic mitral regurgitation. *Circulation* 2003;108(Suppl.1):II116-II121
20. Hung J, Papakostas L, Tahta SA, et al. Mechanism of recurrent ischemic mitral regurgitation after annuloplasty: Continued LV remodeling as a moving target. *Circulation* 2004;110(11 Suppl.1):II85-II90
21. Messas E, Guerrero JL, Handschumacher MD, et al. Chordal cutting: A new therapeutic approach for ischemic mitral regurgitation. *Circulation* 2001;104(16):1958-1963
22. Messas E, Pouzet B, Touchot B, et al. Efficacy of chordal cutting to relieve chronic persistent ischemic mitral regurgitation. *Circulation* 2003;108(Suppl.II):II111-II115
23. Rodriguez F, Langer F, Harrington KB, et al. Cutting second-order chords does not prevent acute ischemic mitral regurgitation. *Circulation* 2004;110(11 Suppl.1):II91-II97
24. Nielsen SL, Timek TA, Green GR, et al. Influence of anterior mitral leaflet second-order chordae tendinae on left ventricular systolic function. *Circulation* 2003;108:486-491
25. Rodriguez F, Langer F, Harrington KB, et al. Importance of mitral valve second-order chordae for left ventricular geometry, wall thickening mechanics, and global systolic function. *Circulation* 2004;110(11 Suppl.1):II115-II122
26. Niczyporuk MA, Miller DC. Automatic tracking and digitization of multiple radiopaque myocardial markers. *Comput Biomed Res* 1991;24:129-142
27. Daughters GT, Sanders WJ, Miller DC, Schwartzkopf A, Mead CW, Ingels NB, Jr. A comparison of two analytical systems from three-dimensional reconstruction from biplane videoradiograms. *Proc Comp Cardiol (IEEE)* 1988;15:79-82
28. Miller GE, Marcotte H. Computer simulation of human mitral valve mechanics and motion. *Comput Biol Med* 1987;17:305-319
29. Goetz WA, Lim HS, Pekar F, et al. Anterior mitral leaflet mobility is limited by the basal stay chords. *Circulation* 2003;107:2969-2974
30. Grande-Allen KJ, Borowski AG, Troughton RW, et al. Apparently normal mitral valves in patients with heart failure demonstrate biochemical and structural derangements: An extracellular matrix and echocardiographic study. *J Am Coll Cardiol* 2005;45:54-61
31. Timek TA, Nielsen SL, Green GR, et al. Influence of anterior mitral leaflet second-order chordae on leaflet dynamics and valve competence. *Ann Thorac Surg* 2001;72:535-540

Meeting discussion

DR. KAREN KUNZELMAN (Lewiston, Maine, USA): We have recently published details of a coupled fluid structure model of the mitral valve that has first- and second-order chords in the multiple branches and the strut chords. We did not assume any curvature a priori, but in response to the atrial and ventricular pressures, the anterior leaflet assumed a shape that had some compound curvature. This was consistent with your model, but the locations may not be the same. I would question your assumption that the change in curvature becomes compressive stress, because when we examined strains at the mid plane, the atrial surface and ventricular surface in those areas of compound curvature, the anterior leaflet was still under tensile stress at all levels. The tensile stress on the atrial surface was less than that at the ventricular surfaces, which is what

changes the curve. A simple analogy is that if you pull a balloon at two points you change its curvature, but it is still under tensile stress. These data raise questions about the shape and function of the anterior leaflet. Cutting the chords does change the shape, but you cannot assume that the change in curvature will introduce compressive stress.

DR. PRAVIN SHAH (Newport Beach, California, USA): The basal portion of the anterior leaflet is in continuity with the mitral aortic curtain. Very often, that portion, the so-called annulus, is either non-existent or is very fragmentary in terms of the 'true annular structure'. My question is how much influence the aortic root dynamics taking place in systole might have on that very small basal segment - it is one-third of the anterior leaflet compared to the remainder. How much influence might that have on the 'complex curvature'?
DR. RODRIGUEZ: Do you mean the anterior mitral

annulus between the left and the right fibrous trigones, which is in continuity with the ventricular-aortic junction?

DR. SHAH: Correct.

DR. RODRIGUEZ: Some elegant studies have been reported showing that during systole, as the ventricular-aortic junction increases in size, so too does somewhat the mitral annulus. We did not characterize curvature in that location, but we believe that the convex aspect of the curvature is related to the saddle horn shape of the mitral annulus. The shape rises from the saddle horn, goes down into the belly of the leaflet, and then billows concave to the left ventricle as you approach the leaflet edge. We did not look at it in transverse section between the fibrous trigones. Does that answer your question?

DR. SHAH: Do all animals have the same degree of saddle horn shape, or do they vary?

DR. RODRIGUEZ: Yes, they do vary, but the saddle horn shape of the mitral annulus is well preserved in all sheep we have studied. This shape was also reported by Dr. Gorman at the University of Pennsylvania.

SIR MAGDI YACOUB (London, UK): Is there a relationship between curvature of the annulus and/or the anterior leaflet and ventricular function? Have you looked at those two points, or is it only related to stress? But is it stress? You have shown that the peak recruitable stroke volume was diminished - is that a separate finding, or is it linked to the change in curvature?

DR. RODRIGUEZ: We did not correlate changes in leaflet shape with observed changes in systolic function, which were attributed to transection of the second-order chords. In our previous studies, Dr. Tibayan examined the effect of leaflet curvature in relation to remodeling of the ventricle post infarction. He showed that the compound curvature was maintained when animals developed chronic ischemic mitral regurgitation, and was able to correlate some changes in geometry to a flattening of the leaflet, although it did maintain its compound curvature. But we have not investigated leaflet curvature in relation to ventricular function, nor do we measure leaflet stress - we only measure leaflet shape.

DR. ROBERT W. M. FRATER (Bronx, New York, USA): Did you place a marker right up under the aortic leaflets in the so-called saddle horn, or was the marker

on the line between the trigones?

DR. RODRIGUEZ: We use a right-angle to find the saddle horn. We pass behind the anterior leaflet and locate the end of the anterior leaflet - that is how we define the mitral annular saddle horn. That is where we sutured the marker, not just between the fibrous trigones.

DR. FRATER: Is there any point in placing a marker in the subaortic area as opposed to the line along which the leaflet actually hinges?

DR. RODRIGUEZ: That would be interesting, but we have not done it. This is the way we have been defining the way our anterior annulus shape.

DR. FRATER: How many second-order chords did you cut?

DR. RODRIGUEZ: We isolated the largest second-order chord that inserted into the belly of the anterior leaflet. In sheep, there were consistently only two large second-order strut chords.

DR. FRATER: There are other second-order chords. All the way from the major chordal insertions down to just a few millimeters above the free edge of the leaflet, there are chordae that can technically be classified as second-order. I suspect that some of the changes that you might consider producing by cutting two large chords are compensated by, just a millimeter below, another set of second-order chordae.

DR. RODRIGUEZ: We absolutely agree, and we did consider that point.

DR. CARLOS DURAN (Missoula, Montana, USA): Just a comment here. We have heard here about the importance of stay chords - what traditionally have been called struts. I think that strut chords is the wrong name, because strut means compression, whereas a stay maintains the mast of a boat with a full roll or a backstay. There are two particularly thick chords that pass to the anterior leaflet, and also two posterior, particularly thick chords that are distinctive. These are found in pigs, sheep and humans, and their presence is fairly consistent. When you cut them, very serious things happen - not only does the anterior leaflet change its shape, but immediately after cutting the cardiac output falls, the dP/dt falls, and the aorto-mitral angle changes. Many geometric changes occur when you cut these chords, because they belong more to the ventricle than to the mitral valve.